J|A|C|S
ARTICLES
Published on Web 02/06/2004

Structure and Dynamics of Au^+ Ion in Aqueous Solution: Ab Initio QM/MM MD Simulations

Ria Armunanto,† Christian F. Schwenk, Hung T. Tran, and Bernd M. Rode*

Contribution from the Department of Theoretical Chemistry, Institute of General, Inorganic and Theoretical Chemistry, University of Innsbruck, Innrain 52a, A-6020 Innsbruck, Austria

Received July 17, 2003; E-mail: bernd.m.rode@uibk.ac.at

Abstract: Structure and dynamics of hydrated Au^+ have been investigated by means of molecular dynamics simulations based on ab initio quantum mechanical molecular mechanical forces at Hartree−Fock level for the treatment of the first hydration shell. The outer region of the system was described using a newly constructed classical three-body corrected potential. The structure was evaluated in terms of radial and angular distribution functions and coordination number distributions. Water exchange processes between coordination shells and bulk indicate a very labile structure of the first hydration shell whose average coordination number of 4.7 is a mixture of 3-, 4-, 5-, 6-, and 7-coordinated species. Fast water exchange reactions between first and second hydration shell occur, and the second hydration shell is exceptionally large. Therefore, the mean residence time of water molecules in the first hydration shell (5.6 ps/7.5 ps for $t^* = 0.5$ ps/2.0 ps) is shorter than that in the second shell (9.4 ps/21.2 ps for $t^* = 0.5$ ps/2.0 ps), leading to a quite specific picture of a "structure-breaking" effect.

1. Introduction

Only few experimental data are available for hydrated Au^+, and no computer simulation results have been reported to our knowledge. Au^+ phosphine complexes have shown antitumor activity,[1] and Au^+ is also of physicochemical interest, due to numerous usages of this metal. The dynamical properties of Au^+ in aqueous solution are of great interest for understanding the physico- and biochemical properties of this metal ion. The results of the paper presented here may stimulate an increased interest to further investigate Au^+ solutions by experimental methods due to some peculiarities predicted.

For the elucidation of details of metal ion solvates, a variety of experimental and theoretical means can be used. For very fast-exchange processes in dilute systems, however, experimental techniques reach their limitations, whereas molecular dynamics simulations can be easily applied for the study of ultrafast dynamics in aqueous solution, provided that their accuracy is high enough. The comparison of classical and QM/MM simulations of metal ions in water and/or ammonia[2−6] have shown the need for a quantum mechanical treatment for at least the first solvation shell to obtain sufficiently accurate data.

The QM/MM formalism including many-body interactions and polarization effects at an ab initio level in the most important region of the system is a necessary compromise, because it is not feasible to treat a representative system of ∼500 particles quantum mechanically. Therefore, the remaining region is treated by molecular mechanics based on an ab initio generated pair plus three-body potential functions.[7] By this approach, the hydration structure of numerous metal ions has been evaluated successfully, and hydration energies and dynamical properties as mean residence times (MRT) and librational and vibrational motions could be obtained.[8,9]

2. Methods

2.1. Potential Functions. The Au^+−water pair potential function was newly constructed using more than 2700 ab initio energy points, defined as:

$$\Delta E^{2bd} = E^{ab}_{MW} - E^{ab}_{M} - E^{ab}_{W} \quad (1)$$

where ab denotes ab initio, MW is the ion−water energy, and M and W mean ion and water, respectively. The minimum energy for the Au^+−H_2O interaction is −28.0 kcalmol^{-1} at a distance of 2.30 Å. More than 12 000 ab initio energy points were used to construct the three-body correction function, and the three-body energies (ΔE^{3bd}_{corr}) were computed as follows:

$$\Delta E^{3bd}_{corr} = (E^{ab}_{WMW} - E^{ab}_{M} - 2E^{ab}_{W}) - \Delta E^{2bd}_{MW}(r_1) - \Delta(r_2) - \Delta E^{2bd}_{WW}(r_3) \quad (2)$$

where ab and 2bd denote ab initio and pair potential energies; MW

† Permanent address: Austrian-Indonesian Center for Computer Chemistry, Chemistry Department, Faculty of Mathematics and Natural Sciences, Gadjah Mada University, Jogjakarta, Indonesia. E-mail: ria.armunanto@uibk.ac.at.

(1) McKeage, M. J.; Maharaj, L.; Berners-Price, S. J. *Coord. Chem. Rev.* **2003**, *232*, 127−135.
(2) Kritayakornupong, C.; Yagüe, J. I.; Rode, B. M. *J. Phys. Chem. A* **2002**, *106*, 10584.
(3) Tongraar, A.; Liedl, K. R.; Rode, B. M. *Chem. Phys. Lett.* **1998**, *286*, 56.
(4) Schwenk, C. F.; Loeffler, H. H.; Rode, B. M. *Chem. Phys. Lett.* **2001**, *349*, 99.
(5) Schwenk, C. F.; Loeffler, H. H.; Rode, B. M. *J. Chem. Phys.* **2001**, *115*, 1080.
(6) Yang, T.; Tsushima, S.; Suzuki, A. *J. Phys. Chem. A* **2001**, *105*, 10439.
(7) Loeffler, H. H.; Yagüe, J. I.; Rode, B. M. *J. Phys. Chem. A* **2002**, *106*, 9529.
(8) Ohtaki, H.; Radnai, T. *Chem. Rev.* **1993**, *93*, 1157.
(9) Inada, Y.; Loeffler, H. H.; Rode, B. M. *Chem. Phys. Lett.* **2002**, *358*, 449.

10.1021/ja037340f CCC: $27.50

Table 1. Optimized Parameters of the Analytical Pair Potential Function Au^+-H_2O

	A (kcal mol^{-1} Å^6)	B (kcal mol^{-1} Å^8)	C (kcal mol^{-1} Å^9)	D (kcal mol^{-1} Å^{12})
Au^+-O	−4534.88	9112.40	5678.65	−21035.05
Au^+-H	−434.59	1664.70	−2709.41	2172.16

and WW indicate ion−water and water−water interactions, respectively; and r_1, r_2, and r_3 correspond to ion−O(1), ion−O(2), and O(1)−O(2) distances. All pair and three-body interaction energies were calculated at the restricted Hartree−Fock (RHF) level with the relativistically corrected LANL2DZ ECP[10] and double-ζ plus polarization[11] basis sets for gold and water, respectively, and fitted to analytical functions using the Levenberg algorithm. The basis set superposition error (BSSE)[12] of the system was examined and found to amount to only 0.08 kcal/mol at the equilibrium distance. The water geometry was kept constant throughout the calculations at experimental gas-phase values of O−H = 0.9601 Å and H−O−H = 104.47°.[13] Oxygen and hydrogen charges were set to −0.6598 and 0.3299,[14] respectively. All ab initio calculations were performed using the Turbomole[15−17] program.

The two-body ab initio energies were fitted to:

$$\Delta E_{\mathrm{Fit}}^{\mathrm{2bd}} = \sum_{i=1}^{3} \frac{q_{\mathrm{M}} q_i}{r_{\mathrm{M}i}} + \frac{A_i}{r_{\mathrm{M}i}^6} + \frac{B_i}{r_{\mathrm{M}i}^8} + \frac{C_i}{r_{\mathrm{M}i}^9} + \frac{D_i}{r_{\mathrm{M}i}^{12}} \qquad (3)$$

where M and i denote Au^+ and oxygen/hydrogen atoms; A, B, C, and D are the optimized parameters, and q represents the atomic charges. The optimized parameters are summarized in Table 1.

The three-body correction energies were fitted to the equation:

$$\Delta E_{\mathrm{Fit}}^{\mathrm{3bd}} = 0.64 \exp[-0.16(r_1 + r_2)] \exp[-0.67 r_3](\mathrm{CL} - r_1)^2(\mathrm{CL} - r_2)^2 \qquad (4)$$

where CL, set to 6.0 Å, is the cutoff limit beyond which three-body terms become negligible.

2.2. Simulation Protocol. The simulation protocol is similar to that in our previous work.[18] The cubic elementary box of 24.8 Å side length contained 1 Au^+ ion and 499 water molecules corresponding to the density of the system of 0.99702 g/cm^3. A canonical *NVT* ensemble at 298.16 K was simulated with periodic boundary conditions,[19] and the temperature was kept constant using the Berendsen algorithm.[20] For water−water interactions, the flexible BJH−CF2 water model was used, consisting of inter- and intramolecular potentials. The time step of the simulation was set to 0.2 fs, which allowed for explicit movement of hydrogens. A cutoff of 12.0 Å was set except for O−H and H−H non-Coulombic interactions, where it was set to 5.0 and 3.0 Å.

2.3. QM/MM Simulations. The QM/MM technique divides the system into the part of major interest, i.e., in the present study the first hydration shell of the cation, treated quantum mechanically, and the rest of the box treated classically as described in detail in several previous publications.[7,18,21] A classical simulation was performed first for 50 ps, and subsequently, the QM/MM simulation was performed for 18.2 ps after 4 ps of reequilibration. The QM radius was set to 3.8 Å, according to the Au−O RDF obtained from the classical simulation, to fully include the first hydration shell.

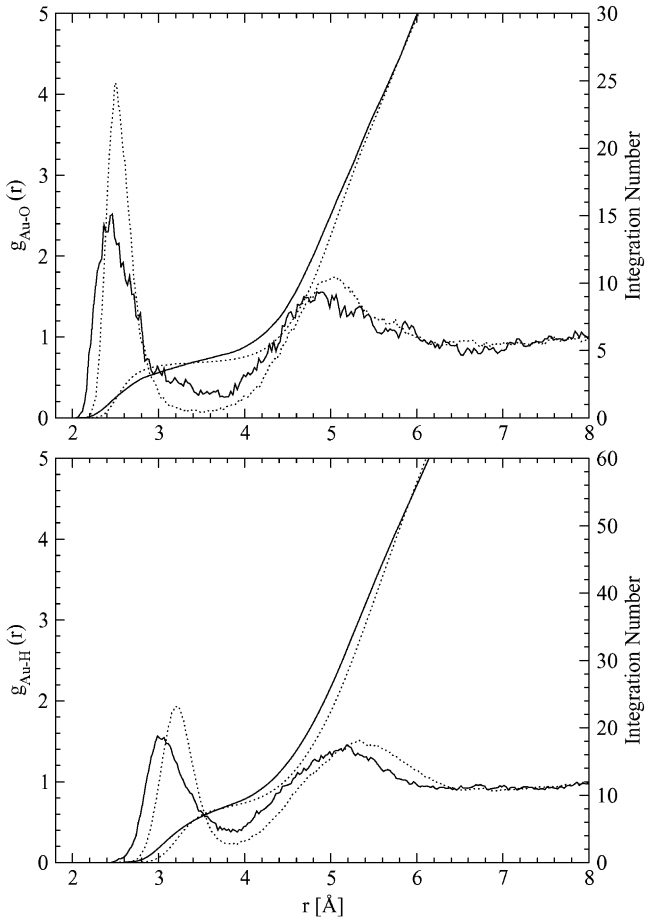

Figure 1. Au−O and Au−H radial distribution functions and their corresponding integration numbers obtained from QM/MM (solid line) and classical (dotted line) simulations.

The evaluation of spectral properties such as librational and vibrational frequencies of water motions was carried out using velocity autocorrelation functions (VACF). The power spectrum of the VACF was calculated by Fourier transformation. Librational and vibrational frequencies of water molecules as well as ion−oxygen motions were computed using the approximative normal coordinate analysis[22] similar to previous work.[21] Six scalar quantities, Q_1, Q_2, Q_3, and R_x, R_y, R_z, defined the symmetric stretching, bending and asymmetric stretching vibrations, and rotations around the three principal axes of the water molecules. The mean residence times (τ) of water molecules in the hydration shells of Au^+ were calculated with the formalism proposed by Impey[23] using a t^* parameter of 2.0 and 0.5 ps.

3. Results and Discussion

3.1. Structural Properties. The Au−O and Au−H radial distribution functions (RDFs), and their running integration numbers obtained from classical and QM/MM simulations are

(10) Hay, P. J.; Wadt, W. R. *J. Chem. Phys*. **1985**, *82*, 270.
(11) Dunning, T. R. J. *J. Chem. Phys*. **1970**, *53*, 2823.
(12) Davidson, E. R.; Feller, B. *Chem. Rev*. **1986**, *86*, 681.
(13) Kuchitsu, K.; Morino, T.; Maeda, M. *Bull. Chem. Soc. Jpn*. **1976**, *49*, 701.
(14) Stillinger, F. H.; Rahman, A. *J. Chem. Phys*. **1978**, *98*, 129.
(15) Ahlrichs, R.; Bär, M.; Horn, H.; Häser, M.; Kölmel, C. *Chem. Phys. Lett*. **1989**, *162*, 165.
(16) Ahlrichs, R.; von Arnim, M. In *Methods and Techniques in Computational Chemistry: METECC-95*; Clementi, E., Corongiu, G., Eds.; STEF-VERLAG: Cagliari, 1995.
(17) von Arnim, M.; Ahlrichs, R. *J. Comput. Chem*. **1998**, *19*, 1746.
(18) Armunanto, R.; Schwenk, C. F.; Rode, B. M. *J. Phys. Chem. A* **2003**, *107*, 3132−3138.
(19) Allen, M. P.; Tildesley, D. J. *Computer Simulation of Liquids*; Oxford University Press: New York, 1987.
(20) Berendsen, H. J.; Grigera, J. R.; Straatsma, T. P. *J. Phys. Chem*. **1983**, *91*, 6269.
(21) Schwenk, C. F.; Loeffler, H. H.; Rode, B. M. *J. Am. Chem. Soc*. **2003**, *125*, 1618−1624.
(22) Bopp, P. *Chem. Phys*. **1986**, *106*, 205.
(23) Impey, R. W.; Maden, P. A.; McDonald, I. R. *J. Phys. Chem*. **1983**, *87*, 5071.

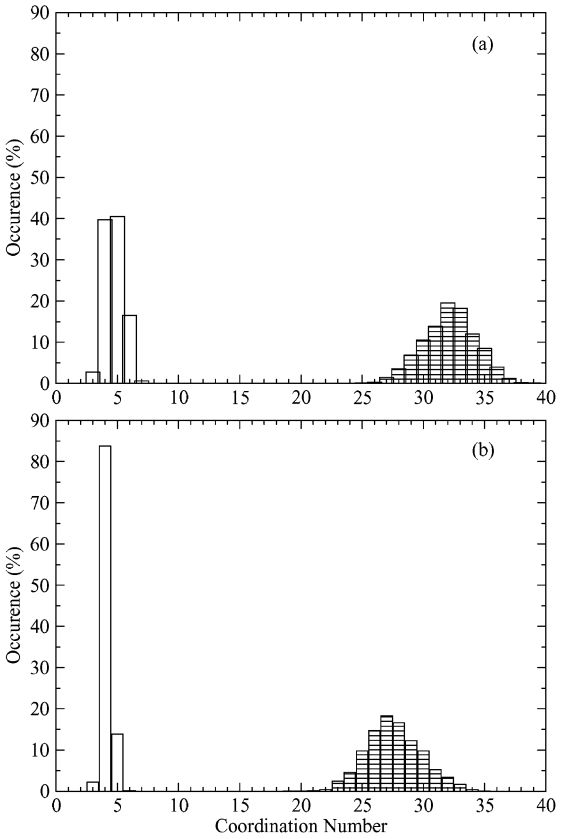

Figure 2. Coordination number distributions of Au^+ in water obtained from (a) QM/MM and (b) classical simulations.

Table 2. Characteristic Values of the Radial Distribution Functions $g_{\alpha\beta}(r)$ for Au^+ in Aqueous Solution Obtained from QM/MM and Classical Simulations, Where r_{M_i} and r_{m_i} Are the Distances in Å of the ith Maxima and Minima of $g_{\alpha\beta}(r)$ and $n_{\alpha\beta}(m_i)$ Is the Average Coordination Number Integrated up to r_{m_i} of the ith Shell

method	α	β	r_{M_1}	r_{m_1}	$n_{\alpha\beta}(m_1)$	r_{M_2}	r_{m_2}	$n_{\alpha\beta}(m_2)$
QM/MM	Au	O	2.45	3.80	4.7	4.9	6.5	33
	Au	H	2.99	3.69	7.8	5.2	6.2	55
classical	Au	O	2.49	3.50	4.1	5.1	6.2	28
	Au	H	3.24	3.91	8.5	5.3	6.5	>65

displayed in Figure 1, and the main structural parameters are listed in Table 2. The first Au−O RDF peak obtained from the QM/MM simulation reaches its maximum at 2.45 Å, and its tailing, particularly displayed by the QM/MM simulation, indicates a high flexibility of the first-shell structure. Between the first and second shells, the Au−O RDF peak never comes close to zero, corresponding to fast intershell water exchange processes. The second Au−O peak reflects a distinct, broad second hydration shell in both simulations. The integration of this peak leads to unusually high numbers of ligands, amounting to 28 and 33 in classical and QM/MM simulations, respectively. This large second hydration shell is also a remarkable difference between Au^+ and Ag^+. For the latter, the second hydration shell consists of only 18 ligands.[18]

The interaction energy for Au^+-H_2O near the end of the second hydration peak, i.e., in the distance range of 6.0−6.5 Å is ∼−3.5 kcal/mol, which is similar to the hydrogen bond energy between ligands. In this region, the orientation of water molecules will frequently change, which can therefore lead to considerable structural irregularities, often associated with a "structure breaking" effect as observed for Cs^+.[24]

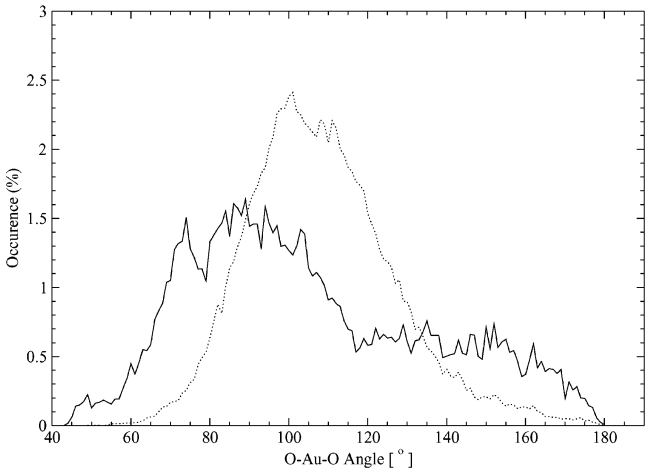

Figure 3. Angular distribution function of $O-Au^+-O$ obtained by QM/MM (solid line) and classical (dotted line) simulations.

Strongly varying first-shell coordination numbers (3−7 H_2O) were observed in the QM/MM simulation, indicating a labile structure of even the first hydration shell (Figure 2). The classical MD simulation shows a more rigid behavior of the first coordination shell (Figure 2) with a strongly preferred 4-fold coordinated species. Coordination numbers 4 and 5 are dominant in the QM/MM simulations, but also smaller amounts of 3-, 6-, and 7-fold coordination occur. Unfortunately, experimental structures, especially EXAFS data, being the best comparable ones due to the low concentration used, are not available yet for Au^+ solutions.

The O−Au−O angle distribution functions (ADF) of the first-shell structure obtained from classical and QM/MM simulations are shown in Figure 3. The classical simulation reflects a rather flexible tetrahedral arrangement of the preferred $Au(H_2O)_4^+$ species, while the quantum mechanical simulation displays a wide spectrum of orientations, corresponding to the observed mixture of species with $n = 3-7$. The larger peak around 90° indicates a preference of square-planar and octahedral arrangements.

The flexibility of the first hydration shell could be visualized by a video clip created from the QM/MM simulation trajectory using the MOLVISION[25] program, and this video clip is available for download at http://www.molvision.com/video clip/Au(I)-water.mpg. The visualization clearly shows the preference of the 4- and 5-fold configurations in the first hydration shell, but also the frequent transitions to other configurations (3-, 6-, and 7-fold). This mixture of several configurations also explains the tailing of the first Au−O peak. "Snapshots" of the simulation showing 3-, 4-, 5-, and 6-fold coordinated species are displayed in Figure 4. The video clip also allows one to follow the movements of the ligands between the first and second shells associated with the changes of the coordination number, which will be discussed in section 3.2.

The hydration energy of Au^+ resulting from the QM/MM simulation of −139 kcal mol^{-1} is identical to the experimental hydration enthalpy value of −140 kcal mol^{-1}.[26] The Au^+ ion has only a small influence on the water geometry in the first

(24) Sacco, A.; Weingärtner, H. *J. Chem. Soc., Faraday Trans.* **1994**, *90*, 849−853.
(25) Tran, H. T.; Rode, B. M. Molvision: Visualization of Chemical Systems Home Page. http://www.molvision.com, section video clips.
(26) Marcus, Y. *J. Chem. Soc., Faraday Trans. 1* **1987**, *83*, 339.

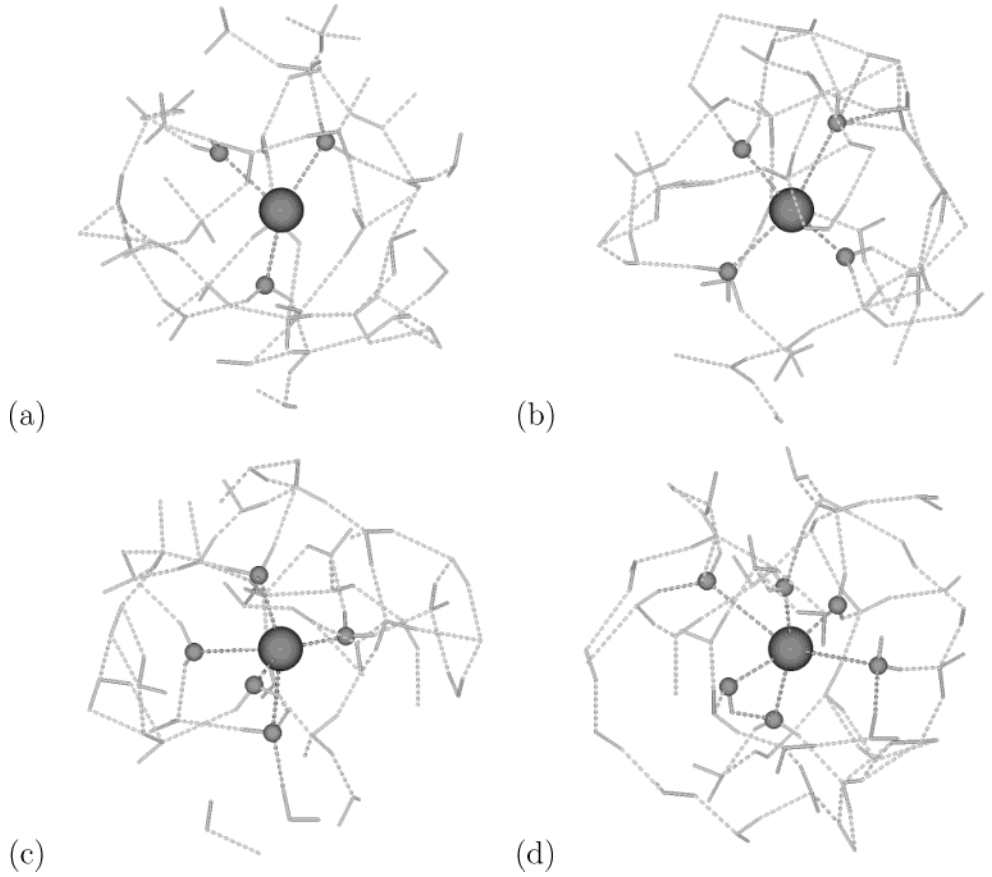

Figure 4. Structures of hydrated Au^+ (first shell, using a cutoff of 6.5 Å) showing coordination numbers of (a) 3, (b) 4, (c) 5, and (d) 6. Hydrogen atoms are not shown explicitly. The big sphere represents the Au^+ ion, and the small-sized ones are oxygens in the first shell.

shell, leading to an elongation of the O−H bond of 0.01 Å and a slightly reduced H−O−H angle. The angle between the Au−O connection vector and the plane formed by O−H vectors defines the tilt angle, and the angle between the Au−O vector and the resulting vector from the sum of O−H vectors has been termed θ angle. The tilt and θ angle distributions obtained from the QM/MM simulation are shown in Figure 5. The broad peaks show the flexibility of the ligand orientations, proving the weak structure-forming ability of Au^+ even for its nearest environment.

3.2. Dynamical Properties. All frequencies in the first shell obtained by the QM/MM simulation were scaled by the standard factor of 0.89,[27,28] since all atomic motions in this shell were generated from the quantum mechanical forces of the HF−SCF wave functions. The weak ion−water interaction causes ligands to be only loosely bound, resulting in a low frequency of the ion−oxygen vibration. The power spectrum of the Au^+−O stretching vibration in the first shell obtained from the QM/MM simulations is displayed in Figure 6. Peaks are observed at 210, 180, and 76 cm^{-1}, which reflects again the presence of different complex species. The corresponding force constants of the QM/MM simulation are 39, 28, and 5.0 N m^{-1}.

The power spectra of VACFs for the librational motions around the axes R_x, R_y, R_z and the vibrational motions for bending frequency Q_2 and stretching frequencies Q_1 and Q_3 obtained from QM/MM simulations are displayed in Figure 7,

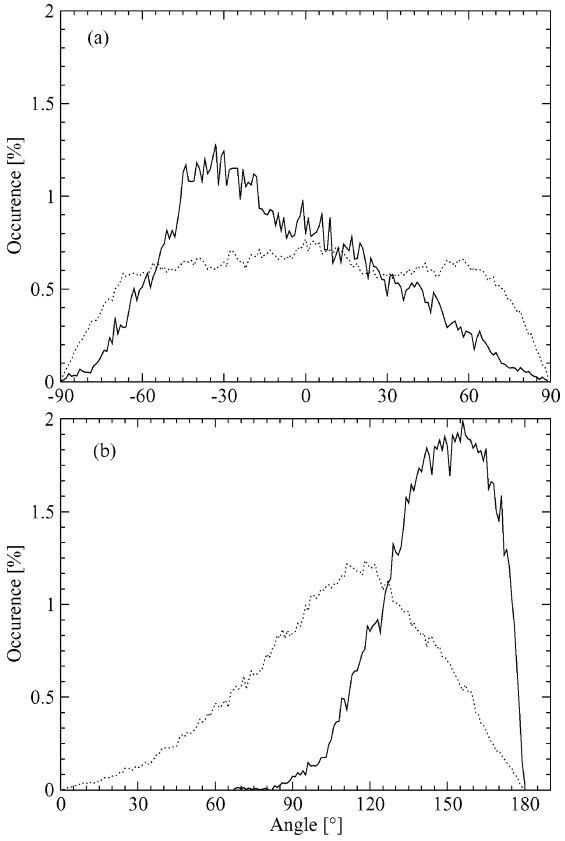

Figure 5. Tilt (a) and θ (b) angle distributions of first (solid line) and second (dotted line) shells obtained from QM/MM simulation.

(27) Scott, A. P.; Radom, L. *J. Phys. Chem.* **1996**, *100*, 16502.
(28) DeFrees, D. J.; McLean, A. D. *J. Chem. Phys.* **1985**, *82*, 333.

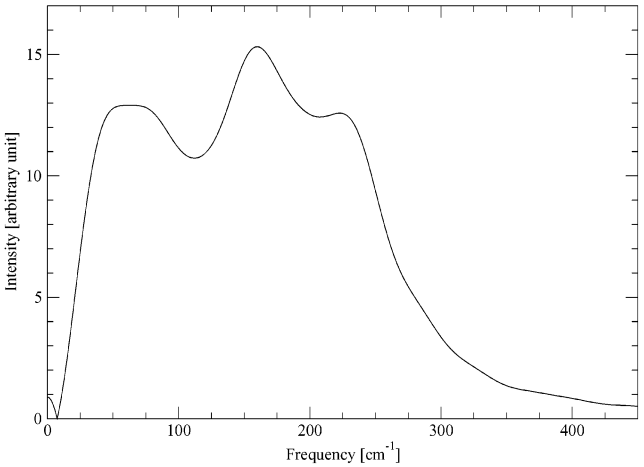

Figure 6. Power spectra of Au^+−oxygen vibrational modes in the first hydration shell obtained by and QM/MM simulations.

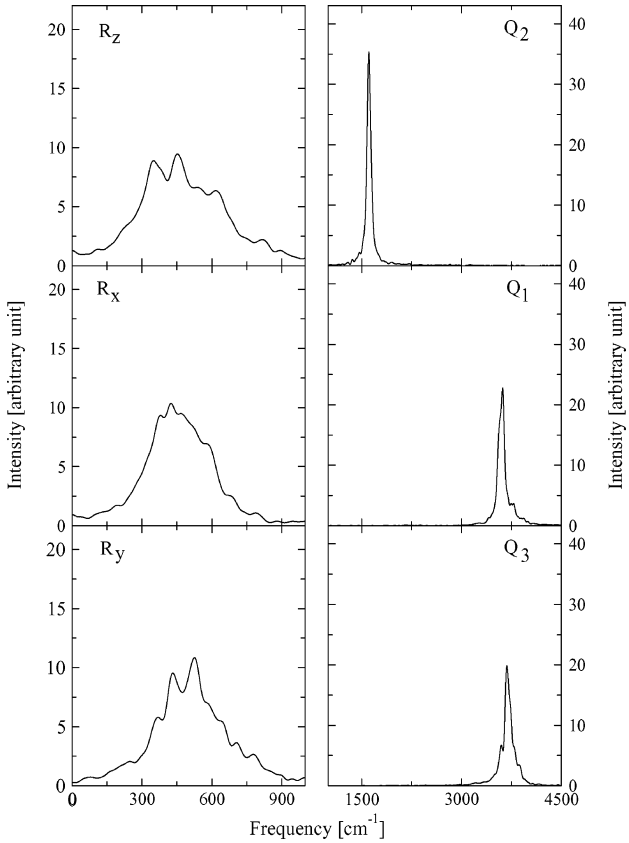

Figure 7. Power spectra of rotational modes R_z, R_x, R_y and vibrational modes Q_2, Q_1, Q_3 for water molecules in the first hydration shell obtained by QM/MM simulations.

and the frequencies obtained by both simulations are summarized in Table 3.

The order $R_z < R_x < R_y$ obtained in the first shell of both simulations is the same for other ions studied in previous simulations.[9,21,29] The QM/MM frequencies of R_z and R_y in the first shell are red-shifted in comparison with the bulk showing an easier rotation around the *z*- and *y*-axes. In contrast, the classical simulation gives blue-shifted values due to a stronger ligand fixation to the ion. The splitted peaks in the QM/MM simulation reflect the presence of different ion−ligand bonds

(29) Tongraar, A.; Liedl, K. R.; Rode, B. M. *J. Phys. Chem. A* **1997**, *101*, 6299.

Table 3. Librational and Vibrational Frequencies of Water Molecules in the First and Second Hydration Shells of the Au^+ Ion and in the Bulk

		frequency [cm^{-1}]					
phase	method	R_Z	R_X	R_Y	Q_2	Q_1	Q_3
first shell	QM/MM[a]	**402**	**425**	**525**	**1608**	**3618**	**3681**
	classical	430	532	642	1695	3361	3450
second shell	QM/MM[e]	**415**	**410**	**540**	**1694**	**3447**	**3558**
	classical	425	430	547	1698	3446	3543
bulk	QM/MM[e]	**415**	**423**	**550**	**1698**	**3448**	**3544**
	classical	410	422	548	1697	3452	3555
liquid[b]					1645	3345	3445
gas[c]					1595	3657	3756
gas[d]					1601	3641	3756

[a] Using scaled value of 0.89; refs 27 and 28. [b] Experimental values in liquid water; ref 31. [c] Experimental values in gas phase; ref 32. [d] Scaled gas-phase vibrational frequencies using the DZP basis set for water; ref 9. [e] Inside the MM region.

Table 4. Reorientational Times of First and Second Order of Water Molecules in the First and Second Hydration Shells, and Bulk of Au^+ in Water Obtained from QM/MM and Classical Simulations

		time [ps]					
phase	method	τ_{1z}	τ_{1x}	τ_{1y}	τ_{2z}	τ_{2x}	τ_{2y}
first shell	QM/MM	5.4	3.8	3.3	1.8	1.6	1.3
	classical	31.0	6.0	6.5	11.9	8.3	6.2
second shell	QM/MM	6.5	7.9	5.0	2.5	3.5	2.2
	classical	8.8	10.6	8.2	3.7	4.3	3.4
bulk	QM/MM	9.3	9.2	6.3	3.7	4.3	3.0
	classical	8.8	8.9	5.9	3.9	4.5	3.1
liquid	BJH[a]	7.7			2.9		
	exptl[b]	7.5			2.5		

[a] Simulation using the CF2−BJH model; refs 21 and 23. [b] Experimental reorientational correlation time of water; ref 8.

in different solvate structures. The stretching frequencies of the first hydration shell obtained by the QM/MM simulation are blue-shifted, whereas the bending frequency is red-shifted in comparison to the bulk. The classical simulation shows an unchanged bending vibration and red-shifts for the stretching vibrations. The second-shell R_x and R_y frequencies are red-shifted as are those in the first shell in comparison with the bulk. This higher mobility is a strong hint toward a structure-breaking effect.[30]

The RTCF values of first (τ_1) and second (τ_2) order in the axes directions of a water molecule are summarized in Table 4. The correlation function for $l = 1$ is related to infrared line shapes and for $l = 2$ to Raman line shapes and NMR relaxation time.[8] The QM/MM results exhibit significantly shorter relaxation times for both first (QM treated) and second (MM treated) hydration shell in comparison with the bulk, which again characterizes Au^+ as a structure-breaking ion. This effect is partly visible from the classical τ_x and τ_y values, whereas the classical τ_{1z} value seems to be rather an artifact of the too-rigid classical model.

3.3. Ligand Exchange Processes. To discuss ligand exchange processes, it seemed of interest to quantify hydrogen bonding between the first and second hydration shells. Table 5 lists

(30) Kritayakornupong, C.; Plankensteiner, K.; Rode, B. M. *Chem. Phys. Lett.* **2003**, *371*, 438−444.
(31) Murphy, W. F.; Bernstein, H. J. *J. Phys. Chem.* **1972**, *76*, 1147.
(32) Eisenberg, D.; Kauzmann, W. *The Structure and Properties of Water*; Oxford University Press: Oxford, 1969.
(33) Bopp, P.; Dietz, W.; Heinzinger, K. *Z. Naturfosch., A* **1979**, *34*, 1424.
(34) García, A. E.; Stiller, L. *J. Comput. Chem.* **1993**, *14*, 1396.

Table 5. Hydrogen Bonds Formed between Water Molecules in the First and the Second Hydration Shells of Au^+ in Aqueous Solution, Obtained by QM/MM Simulation

no. of ligands	NHB[a]	LHB[b] [Å]
3	1.70	2.03
4	2.47	2.00
5	2.29	1.97
6	2.19	1.89

[a] Average number of hydrogen bonds. [b] Average length of hydrogen bonds.

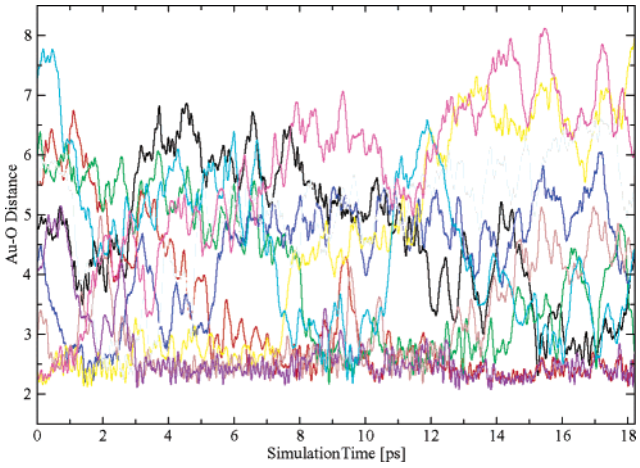

Figure 8. Variation of ion−oxygen distances during the QM/MM simulation, showing numerous exchange processes between the first and second hydration shells.

the results for the various $Au(H_2O)_n^+$ species observed in the QM/MM simulation. Except for the tri-coordinated species, which can rather be seen as a transition state, all hydrates form on average more than two H bonds, i.e., they are associated with more than two ligands of the second shell. This is only possible due to a very flexible orientation of second-shell ligands, allowing $[H-O-H]^{II}\cdots[OH_2]^{I}$ bonds as well. This flexible structure should also allow an easy exchange of liquids between both shells.

Ion−water distance plots of the QM/MM simulation are depicted in Figure 8. Twenty-five water molecules have been involved in exchange processes between the first and second hydration shells, illustrating the expected ease of ligand migration.

The mean residences time of a ligand is defined as the average lifetime of a water molecule in a given coordination shell. The mean residence times of water molecules (τ) in both hydration shells have been calculated according to Impey,[23] using $t^* = 2.0$ ps. The choice of $t^* = 2.0$ ps is rather arbitrary but more or less conventional[23,24] and might be questioned for the case of such fast-exchanging hydration shells. For this reason, we have performed the same calculations also for $t^* = 0.5$ ps, and the corresponding results are given as second values. For the QM/MM simulation, the mean residence time in the first shell (7.5 ps/5.6 ps) is smaller than that in the second hydration shell (21.2 ps/9.4 ps). Mean residence times obtained from the classical simulations are significantly higher for both shells and do not reproduce this particular "structure breaking" effect.

4. Conclusions

The monovalent ion of gold displays a number of interesting features, among which an extremely labile first hydration shell and an exceptionally large second shell lay the foundation for other properties, such as a ligand exchange between both shells, which is faster than the exchange between the second shell and the bulk. This leads to a specific "structure breaking" effect of this ion: on one hand, near the ion the mobility of ligands is strongly enhanced, and on the other hand, a bulky second hydration sphere represents a far-reaching perturbation of the solvent structure. Au^+ in water appears to be a highly interesting system, therefore, for experimental investigations, although the expected simultaneous presence of several species and the extremely fast change of coordination numbers will make the modeling for the interpretation of spectral data a challenging task.

Acknowledgment. Financial support for this work from the Austrian Science Foundation (FWF) (project P16221-N08) and a scholarship of the Austrian Federal Ministry for Foreign Affairs to R.A. are gratefully acknowledged.

JA037340F